PROSTHETICS

Powered knee and ankle prosthesis with indirect volitional swing control enables level-ground walking and crossing over obstacles

Joel Mendez, Sarah Hood, Andy Gunnel, Tommaso Lenzi*

Powered prostheses aim to mimic the missing biological limb with controllers that are finely tuned to replicate the nominal gait pattern of non-amputee individuals. Unfortunately, this control approach poses a problem with real-world ambulation, which includes tasks such as crossing over obstacles, where the prosthesis trajectory must be modified to provide adequate foot clearance and ensure timely foot placement. Here, we show an indirect volitional control approach that enables prosthesis users to walk at different speeds while smoothly and continuously crossing over obstacles of different sizes without explicit classification of the environment. At the high level, the proposed controller relies on a heuristic algorithm to continuously change the maximum knee flexion angle and the swing duration in harmony with the user's residual limb. At the low level, minimum-jerk planning is used to continuously adapt the swing trajectory while maximizing smoothness. Experiments with three individuals with above-knee amputation show that the proposed control approach allows for volitional control of foot clearance, which is necessary to negotiate environmental barriers. Our study suggests that a powered prosthesis controller with intrinsic, volitional adaptability may provide prosthesis users with functionality that is not currently available, facilitating real-world ambulation.

INTRODUCTION

Most available knee prostheses are energetically passive devices with limited ability to reproduce the behavior of the healthy biological knee (*1*). In the simplest devices, the biomechanical behavior of the healthy knee joint is approximated by friction elements or hydraulic dampers (*2*). More advanced knee prostheses use a microcontroller to change the knee damping within the gait cycle. These microprocessor-controlled knees allow for variable cadence (*3*) while improving stance stability (*4*) and reducing metabolic cost of walking compared with friction and hydraulic knees (*5*, *6*). Despite these improvements, ambulation is slower, less stable, and less efficient for individuals with above-knee amputation than for non-amputee individuals (*7*). Moreover, negotiating common environmental barriers—such as curbs, stairs, or uneven surfaces—requires unnatural, destabilizing movements, such as residual hip circumduction and plantar flexion of the sound ankle [i.e., vaulting (*8*)], to compensate for the missing prosthesis knee flexion (*8*–*10*). Thus, alternative and improved prosthesis technologies are necessary to address the needs of individuals with an above-knee amputation.

In contrast to passive prostheses, powered prostheses can actively regulate joint movements using battery-powered servomotors. To accomplish this goal, powered prostheses typically use controllers that aim to replicate the behavior of the healthy leg across different ambulation activities. One common control method consists of dividing the gait cycle into segments that are characteristic of the nominal gait pattern, such as stance and swing (*11*). In swing, the trajectory of the powered prosthetic joint is often determined by joint impedance parameters such as stiffness, damping, and equilibrium point, which are tuned by the experimenter to imitate the nominal knee joint trajectory (*12*, *13*). To accomplish this goal, swing must be divided into two segments with different impedance parameters. Furthermore, individual-specific tuning of impedance parameters is necessary to change the swing timing as needed to walk at different speeds (*14*, *15*). Despite their robustness, impedance-based controllers have limited adaptability, making it hard to adapt the swing trajectory to the user's needs.

Position-based controllers have been recently proposed to simplify the tuning procedure and provide more flexibility over the powered prosthesis behavior. Rather than using a set of impedance parameters, position-based controllers define the whole swing trajectory either as a continuous function of time (*11*, *16*, *17*) or as residual-limb movements (*18*, *19*). Using this approach, the desired position trajectory can be conveniently extracted from the analysis of non-amputee biomechanics, which avoids the need for manual tuning (*20*). The desired trajectory can then be stored in look-up tables, encoded using parametric functions (*21*), or obtained online using minimum-jerk programming (*17*). Position-based controllers have been used successfully for different locomotion tasks such as variable-speed walking (*17*), variable inclines (*22*), and stair climbing (*21*, *23*, *24*). However, this control approach lacks the ability to adapt the prosthesis trajectory outside of the preprogrammed gait pattern. Thus, a specific trajectory must be preprogrammed for every possible activity that the user wants to perform. In addition, an intention-detection algorithm must be available to timely and accurately detect the user's intended activity to trigger the switch between different activity-specific trajectories. Because of these limitations, available position-based controllers are not suitable to traverse environmental barriers such as curbs and uneven surfaces.

Classification-based controllers have been proposed to achieve ambulation over different terrains. The basic idea is to use separate controllers for different environmental conditions, which must be detected by an online classifier. The detection of the ambulation activity intended by the user and of the environmental obstacles or constraints can rely on a combination of mechanical sensors (*25*), electromyography (*26*, *27*), sonomyography (*28*), lasers (*29*), or computer vision (*30*, *31*). These classification-based controllers

Department of Mechanical Engineering and Utah Robotics Center, University of Utah, Salt Lake City, UT, USA.
*Corresponding author. Email: t.lenzi@utah.edu

were originally developed for detecting ramps and stairs and, more recently, have been proposed for obstacle navigation (*32*). Close to 100% online accuracy is necessary for these classification-based controllers to work properly because both a false positive and a false negative may result in dangerous behavior of the powered prosthesis, potentially causing the prosthesis user to fall (*33*). Moreover, because of the high interindividual and environment variability, the machine learning algorithms performing the classification require extensive individual-specific labeled datasets for training (*25*, *34*). Labeled data collection must be conducted in a controlled environment under the supervision of highly trained personnel. Thus, open challenges remain in obtaining an accuracy that is conducive to use in the community and in the training of the classification algorithms.

Here, we present an alternative control paradigm for powered prostheses that enables adapting the swing trajectory as necessary to traverse environmental barriers. Rather than aiming to classify the intended activity and switching between numerous pretuned, individual-, and activity-specific controllers, we propose using a single controller that continuously adapts the movements of the powered prosthesis based on the movements of the residual limb without an explicit classification of the environmental constraints. We hypothesize that such a continuous modulation will enable individuals with above-knee amputations to volitionally change foot clearance as necessary to traverse barriers. We tested this hypothesis by asking three participants with a unilateral above-knee amputation to cross over obstacles of different sizes while walking on level ground and on a treadmill at different speeds with a powered knee and ankle prosthesis and with their prescribed passive prostheses without compensatory movements (Movie 1). Three non-amputee individuals were enrolled in the study as a control group. A prosthesis controller with this intrinsic adaptability may provide functionality that is not currently available to powered prosthesis users.

RESULTS

Simulations

Volitional control is indirectly obtained using the orientation of the user's residual limb to modulate the prosthesis trajectory in swing. A finite-state machine divides the swing movement into two parts, namely, swing 1 to swing 2. Swing 1 starts when the foot is lifted from the ground and ends when the thigh angle (θ_{thigh}) exceeds a threshold. The desired maximum knee flexion angle (θ^{des}_{final}) in swing 1 is determined by the integral of the residual limb orientation with respect to gravity (θ_{thigh}), computed from the start to the end of swing 1. Thus, the desired final maximum knee flexion angle in swing 1 (θ^{des}_{final}) increases when the residual limb is positioned back or when it is slowly moved forward during swing 1. Given a desired maximum knee flexion angle (θ^{des}_{final}) and swing 1 duration, the swing trajectory is continuously optimized using minimum jerk (*17*). The desired maximum knee flexion (θ^{des}_{final}) in swing 1 does not necessarily match the peak of the desired knee flexion across the whole swing. Furthermore, the thigh threshold for transition between swing 1 and swing 2 (θ^{ths}_{thigh}) is not fixed but rather increases proportionally to the desired peak knee flexion (θ^{des}_{final}) in swing 1. Because of this variable threshold (θ^{ths}_{thigh}), the transition between swing 1 and swing 2 can happen at a different time within the swing, although the desired duration of swing 1 (T_{sw1}) is constant. Thus, using the proposed algorithm, a new trajectory can branch off from the swing trajectory originally programmed at toe-off depending on the movement of the user's residual limb. The prosthesis knee swing trajectory can therefore be modulated by the users through their residual limb, potentially enabling variable foot clearance.

The behavior of the proposed controller is demonstrated by the simulations in Fig. 1. Varying the transition points between swing 1 and

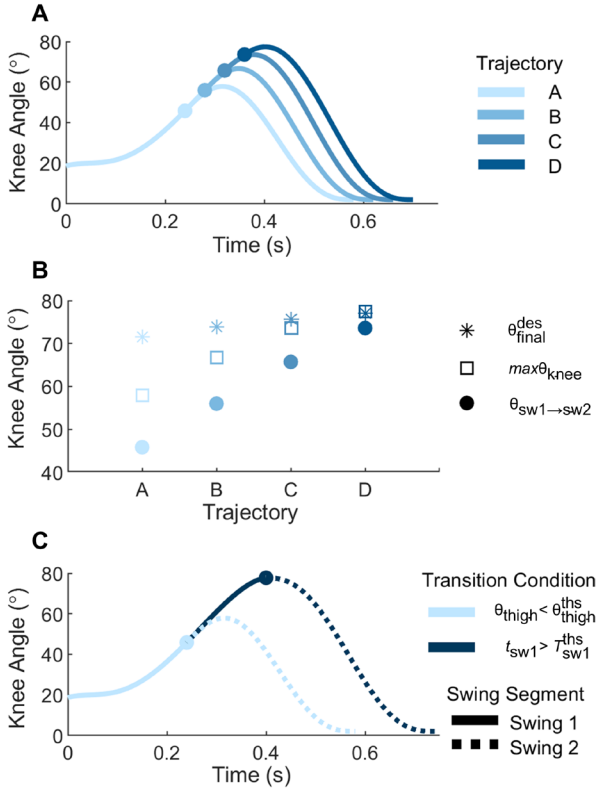

Fig. 1. Simulations of the proposed swing controller. (**A**) Swing trajectories (A to D) for four possible transition points between swing 1 and swing 2 are shown using solid lines with different colors. The transition points are shown using circle markers. (**B**) Desired knee maximum in swing 1 (θ^{des}_{final}), actual knee maximum ($max\theta_{knee}$), and knee angle at the transition between swing 1 and swing 2 ($\theta_{sw1\rightarrow sw2}$) for four simulated trajectories (A to D). (**C**) Swing trajectories for two transition points determined by the thigh position falling below a variable threshold value ($\theta_{thigh} < \theta^{ths}_{thigh}$; light blue) and the time in swing 1 elapsing a variable timeout condition ($t_{sw1} > T^{ths}_{sw1}$; dark blue). The solid line shows the desired position trajectory in swing 1; the dashed line shows the desired position trajectory in swing 2.

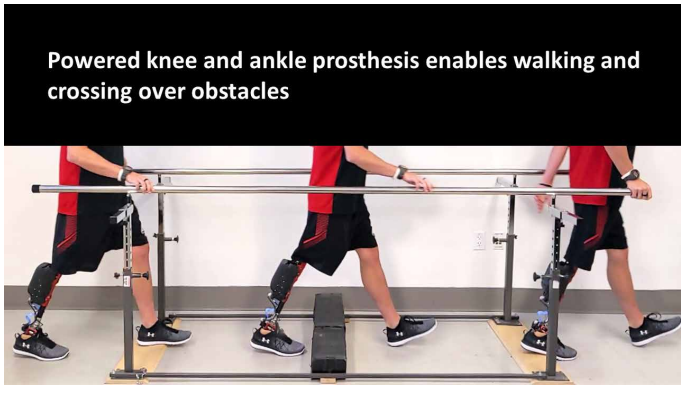

Movie 1. Summary.

swing 2 (circle markers) results in a modulation of the swing trajectory (solid lines with different colors, Fig. 1A). Specifically, a later transition point results in a higher knee flexion angle ($\max\theta_{knee}$) and a longer overall duration of swing (Fig. 1, A and B). The control system transitions between swing 1 and swing 2 even whether the desired peak of knee flexion in swing 1(θ^{des}_{final}) is not achieved. Thus, the maximum knee flexion (θ^{des}_{final}) in swing 1 does not necessarily match the actual maximum of the desired knee swing trajectory ($\max\theta_{knee}$), which can be achieved in swing 2 (Fig. 1B). However, if the transition between swing 1 and swing 2 is due to the elapsed time in swing 1, exceeding a defined threshold, i.e., timeout condition (dark circle marker in Fig. 1C), then the desired peak knee flexion (θ^{des}_{final}) matches the actual peak of the knee trajectory (dark solid line in Fig. 1C). As a result, the transition between swing 1 and swing 2 can happen at a different time within the gait cycle, different knee flexion angles, and different orientations of the user's residual limb. Thus, the proposed variable transition condition between swing 1 and swing 2 enables the powered knee to perform different swing trajectories, theoretically allowing for volitional variations of foot clearance while still maximizing smoothness.

Experiments

The functionality of the proposed controller was measured by observing its performance during a series of tests. In the first test, participants walked back and forth at their self-selected speed on a 4-m walkway, including starting and stopping, while an obstacle was placed in the middle of the walkway. Three different obstacles sizes were used in different trials and are denoted as small (10 cm by 80 cm by 6 cm), medium (15 cm by 80 cm by 10 cm), and large (30 cm by 80 cm by 20 cm). A representative test with one individual with an above-knee amputation (AK03) crossing over the medium-sized obstacle is shown in Fig. 2A. As can be seen in Fig. 2B, the individual performs three consecutive strides with the obstacle being crossed in the second stride with the sound side first. A video of the participants performing the test can be found in movie S1. As can be seen in Fig. 2C, the gait pattern changes considerably when the participant crosses over the obstacle. Specifically, the range of motion of the hip joint (solid yellow line, Fig. 2C) increases from 34° and 39° for the first and last stride, respectively, to 51° for the obstacle-crossing stride. As a result, a 46% longer stride is taken when crossing the obstacle (x axis, Fig. 2C). The maximum knee flexion (solid blue line, Fig. 2C) is 56°, 94°, and 64° for the first, second, and third stride, respectively. Thus, when crossing over the obstacle, the prosthesis achieves a 68% larger maximum knee flexion. As expected, the ankle kinematics is not visibly affected by the presence of the obstacle (solid red line, Fig. 2C). The peak of foot clearance increases from 0.06 and 0.02 m in the first and third stride, respectively, to 0.67 m for the third stride (solid black line, Fig. 2C). Thus, when crossing over the obstacle, the participant holds back the residual limb longer, causing the unified controller to increase the maximum knee flexion angle and, consequently, the foot clearance.

By analyzing the gait kinematics during the level-ground test with and without obstacles, we can assess the ability of a participant to voluntarily change foot clearance. The analysis of the powered knee

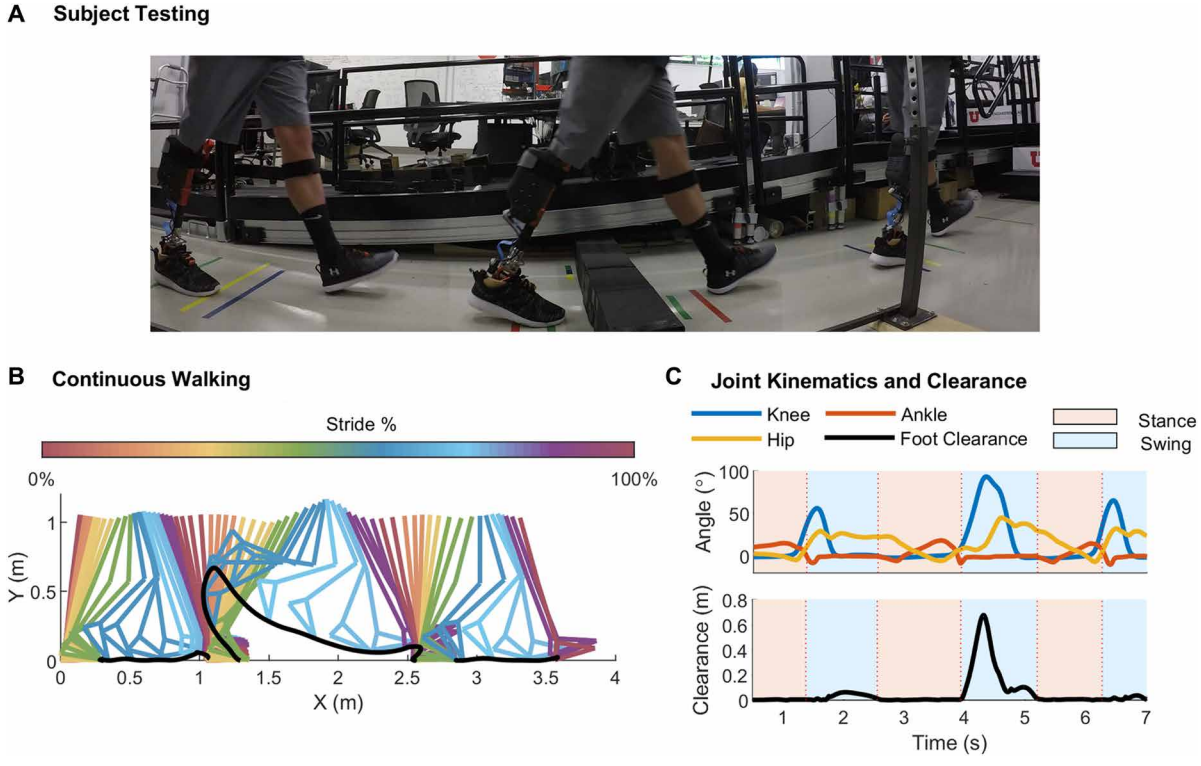

Fig. 2. Continuous modulation of knee flexion and foot clearance with volitional walking controller. (**A**) Overlaid still frames extracted from the video of one participant with an above-knee amputation performing the level-ground obstacle crossing test with the medium-sized obstacle. The source video is available in movie S1. (**B**) Cartesian position of powered prosthesis and residual limb resulting from one participant (AK03) crossing over the medium obstacle at a self-selected speed. The participant performed three strides with the obstacle being crossed in the second stride while leading with the sound side. (**C**) Joint kinematics and foot clearance from one participant (AK03) crossing over the medium obstacle at a self-selected speed.

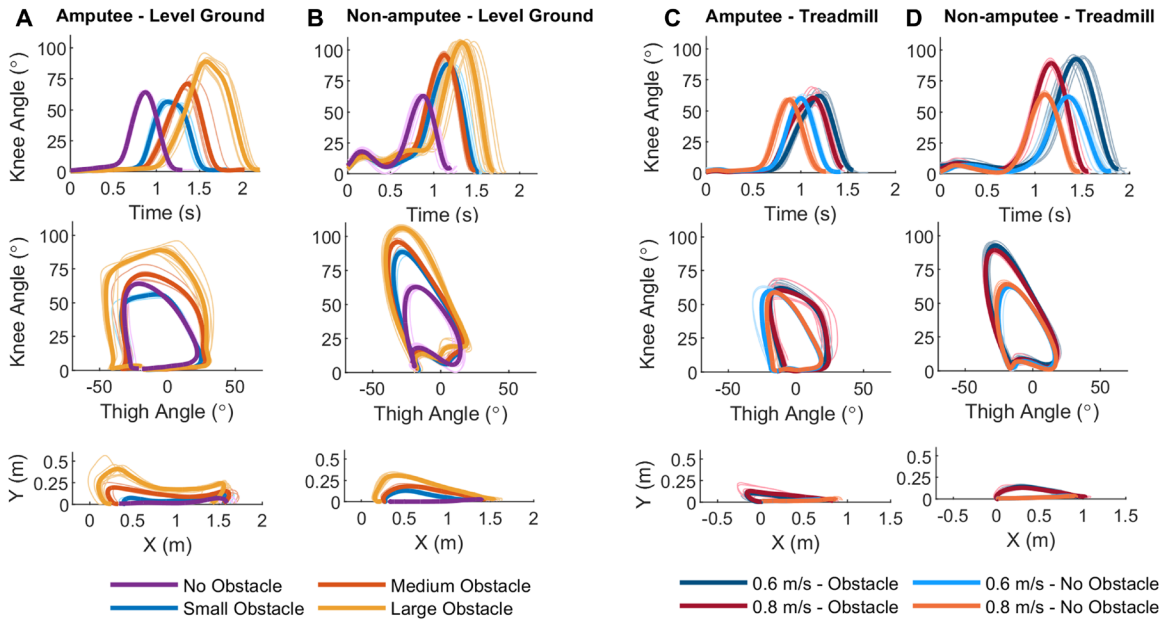

Fig. 3. Resulting leg kinematics with volitional walking controller. (**A**) Level-ground test with AK01. No obstacle (purple), small obstacle (blue), medium obstacle (red), and large obstacle (yellow). (**B**) Level-ground test with AB04. No obstacle (purple), small obstacle (blue), medium obstacle (red), and large obstacle (yellow). (**C**) Treadmill test with AK02. Obstacle (0.6 m/s; dark blue), obstacle (0.8 m/s; dark red), no obstacle (0.6 m/s; light blue), and no obstacle (0.8 m/s; orange). (**D**) Treadmill test with AB04. Obstacle (0.6 m/s; dark blue), obstacle (0.8 m/s; dark red), no obstacle (0.6 m/s; light blue), and no obstacle (0.8 m/s; orange).

kinematics for representative amputee (AK01) and non-amputee participants (AB04) shows that the stride duration is generally longer in the presence of an obstacle and that it increases with the obstacle size (Fig. 3, A and B, and table S1). Similarly, the maximum knee flexion increases with the obstacle size, although it is smaller for the small obstacle test than for the test with no obstacle (table S1). Specifically, the stride duration is 41% longer for the non-amputee participant and 69% longer for the amputee participant. Moreover, the maximum knee flexion for the taller obstacle is 68 and 38% higher than that of the smaller obstacle for the non-amputee and the amputee participant, respectively. For the amputee participant, the inversion of the movement between knee flexion and extension (Fig. 3A) is generally slower when crossing over the obstacle, showing a rather flat region for the small (solid blue line) and large obstacle (solid yellow line). The phase analysis for the above-knee participant (Fig. 3A) shows that the timing between the residual limb motion (i.e., thigh angle, x axis) and the powered knee angle (i.e., y axis) changes when the participant crosses over the obstacle. Specifically, during swing 1 (i.e., positive thigh angle) the knee angle is generally larger when crossing over the obstacle than when no obstacle is present. The phase analysis for the non-amputee participant (Fig. 3B) is similar to that of the amputee participant. However, the non-amputee participant appears to experience a smaller range in thigh motion (i.e., 63°) compared with that of the amputee participant (i.e., 75°). In addition, the non-amputee participant begins knee flexion sooner with thigh motion, whereas the above-knee amputee's knee angle does not appear to change with thigh motion initially. Last, larger foot clearance is observed for both participants when crossing obstacles of increasing sizes (Fig. 3, A and B, and table S1). The foot clearance was up to 10 cm larger for the amputee than the non-amputee participant. Thus, with the proposed swing controller, the participant can voluntarily change the powered knee kinematics and foot clearance as necessary to walk over ground and cross over obstacles of different sizes at the preferred walking speed.

The performance of the proposed swing controller under continuous walking is demonstrated by participants walking on a treadmill at two different speeds (i.e., 0.6 and 0.8 m/s) while an experimenter manually dropped 6-cm-tall obstacles on the belt in the path of the powered prosthesis. The analysis of the knee kinematics (Fig. 3C) for one representative amputee participant (AK02) shows that the stride duration is generally longer for the slower walking speed (i.e., dark and light blue lines) than the faster walking speed (dark red and orange lines). In addition, for the same walking speed, the stride duration is longer when the participant crossed the obstacle (dark blue and dark red lines) than when no obstacle is encountered (orange and light blue lines). At the slower speed (0.6 m/s), the maximum knee flexion is 60.4° ± 2.1° without an obstacle and 64.0° ± 2.3° with an obstacle. At the faster speed (0.8 m/s), the maximum knee flexion is 60.0° ± 0.9° when no obstacle is encountered and 61.1° ± 6.1° when an obstacle is encountered. In comparison, for the non-amputee participant (AB04; Fig. 3D) walking at the slower speed (0.6 m/s) the maximum knee flexion is 62.4° ± 1.6° without an obstacle and 92.7° ± 2.3° with an obstacle. At the faster speed (0.8 m/s), the maximum knee flexion is 64.1° ± 1.5° when no obstacle is encountered and 89.3° ± 2.4° when an obstacle is encountered by the non-amputee participant. Stride duration is 4 and 8% longer when crossing the obstacle at 0.6 m/s for the non-amputee and amputee participant, respectively. In comparison, stride duration is 9 and 13% longer when crossing the obstacle at 0.8 m/s for the non-amputee and amputee participant, respectively. The phase analysis (i.e., knee angle versus the thigh angle) for the above-knee amputee participant shows that timing of the knee and thigh movements is altered when an obstacle is crossed (Fig. 3C). In swing 1 (i.e., positive thigh angle), the knee angle tends to be larger when an obstacle is crossed (dark

red and dark blue lines). On the other hand, the phase analysis shows a smaller range of motion of the thigh for the amputee (i.e., 44°) than the non-amputee participant (i.e., 55°). Moreover, the non-amputee participant shows a larger thigh flexion angle (8.9° on average) and a smaller thigh extension angle (3.5° on average) than the amputee participant. For both, the phase plots are not visibly affected by the treadmill speed (Fig. 3, C and D). For the amputee participant, the altered timing of the knee and thigh movements produce a larger foot clearance (i.e., +261% for the slow treadmill speed and +206% for the fast treadmill speed) when crossing the obstacle. Thus, with the proposed controller, the participant can walk at the two different speeds imposed by the treadmill with and without crossing over obstacles.

The analysis of the group averages of joint kinematics for non-amputee and amputee participants performing the same cross-over obstacle tests provides further insights into the behavior of the proposed volitional controller. The knee kinematics of the passive prosthesis, the powered prosthesis, and the non-amputee biological leg are fairly similar when no obstacle is encountered (Fig. 4), matching closely in swing (60 to 100% of the gait cycle). In contrast, there are noticeable differences in the knee kinematics when participants cross over obstacles (table S1). Overall, the maximum knee flexion angle tends to be greater for non-amputee participants than for participants with an above-knee amputation using the powered prosthesis. In the level-ground walking tests (Fig. 4, A to D), there is a difference of 26.3°, 16.7°, and 15.7° for the small obstacle, medium obstacle, and large obstacle, respectively. However, when no obstacle is encountered, both groups reach similar maximum knee flexion with a 0.4° difference being recorded. The difference in maximum knee flexion is larger for the treadmill tests (Fig. 4, E and F), with it reaching 20.8° and 25.7° for the 0.6 and 0.8 m/s speed, respectively. In contrast, the knee flexion angle decreases when an obstacle is encountered with the passive prosthesis, causing the foot to impact on the obstacle (Fig. 4, B to D). Further insights can be gained from the thigh and hip kinematics. Without obstacles, the thigh is, on average, 3.3° ± 5.1° more extended for the amputee group using the powered prosthesis than the non-amputee group (Fig. 4A). This difference in thigh orientation, which is visible in both stance and swing phase, increases to about 7.1° ± 1.6° when participants cross over obstacles (Fig. 4, B to F). Although less evident, the hip joint kinematics also shows lower extension for the amputee than the non-amputee group when no obstacle is presented (−2.5° ± 4.8°; Fig. 4A) and when crossing over obstacles (−3° ± 3.1°; Fig. 4, B to F). However, the range of the thigh angle is bigger (2.1°), whereas the range of the hip angle is smaller (−2.4°) for the amputee group than the non-amputee group. There are no visible differences in the thigh kinematics of the passive and powered prosthesis in stance phase. Thus, complex postural and joint adaptation are involved when ambulating on different terrains and crossing obstacles of different sizes.

By focusing on the level-ground tests with obstacles (Fig. 4, B to D), we can see that the maximum knee flexion tends to occur later in the gait cycle for non-amputee participants than for participants with an above-knee amputation. On average, the above-knee group

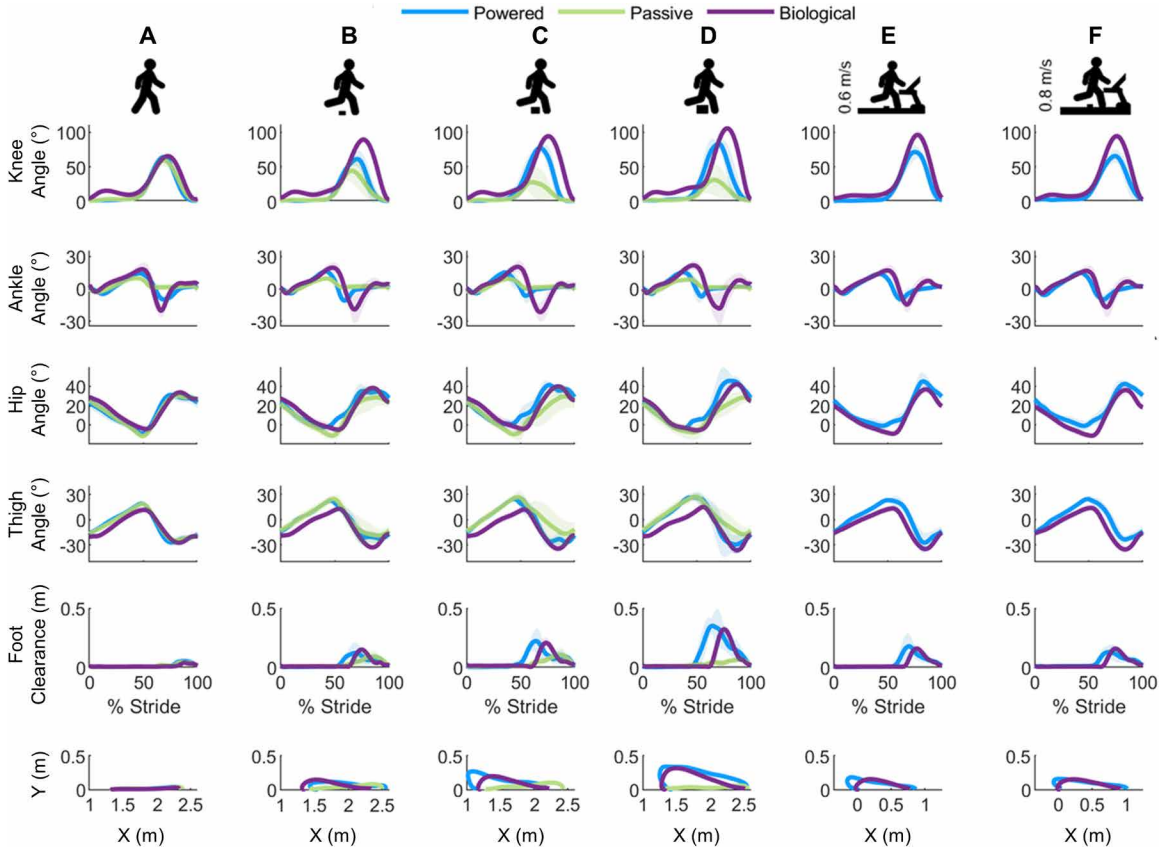

Fig. 4. Comparison between amputee participants using a powered prosthesis, (blue), amputee participants using a passive prosthesis (green), and non-amputee participants (purple) throughout six different tests. (**A**) No obstacle. (**B**) Small obstacle. (**C**) Medium obstacle. (**D**) Large obstacle. (**E**) Treadmill (0.6 m/s). (**F**) Treadmill (0.8 m/s).

reaches their maximum knee flexion at 68 ± 1% of stride whenever they cross any type of obstacle on level ground. The non-amputee participants, on the other hand, reach their maximum knee flexion at 77 ± 1% of stride. When no obstacle is encountered, the above-knee amputee group reach their maximum flexion at 68 ± 1% of stride, whereas the non-amputee participants reach maximum flexion at 72 ± 1% of stride. The timing of the knee flexion is more similar during the treadmill tests, where participants with an above-knee amputation reach their maximum flexion at an average of 75 ± 1% of stride and non-amputee participants reach their maximum flexion at an average of 77 ± 1% of stride. Moreover, in non-amputee individuals, heel strike happens as soon as the knee is fully extended, whereas individuals with an above-knee amputation tend to delay heel strike. During level-ground walking with no obstacle (Fig. 4A), knee extension is completed at 91 ± 1% of stride among the above-knee amputation group. On the other hand, for small, medium, and large obstacle tests (Fig. 4, B to D), knee extension ends at 89 ± 4, 88 ± 3, and 90 ± 5% of stride, respectively. The heel strike delay is less pronounced during the treadmill test (Fig. 4, E and F, where extension ends at 96 ± 2% of stride and 95 ± 4% of stride for the slower and faster walking speeds, respectively. The observed time delay can be also seen in the ankle kinematics.

The analysis of foot clearance as a function of the normalized stride time shows consistently higher variability (shaded areas) for the above-knee group than for the non-amputee group. In contrast, the two groups show similar average trajectories (solid lines), noticeably, with the same time delay for the knee and ankle kinematics. The Cartesian representation of the foot clearance shows that individuals with amputations tend to have higher foot clearance at the beginning of swing, when the foot rises from the ground. In contrast, a similar foot clearance is observed in the two groups at the point where the obstacle is located. Thus, non-amputee participants and participants with an above-knee amputation show different joint kinematics but similar foot clearance when walking and crossing over obstacles.

The proposed swing controller is further analyzed by comparing the maximum knee flexion with maximum foot clearance between different groups (i.e., non-amputee, above-knee) and tests (i.e., small, medium, large, slow, and fast). Similar to non-amputee participants, above-knee participants using the powered prosthesis increase both the maximum knee flexion (Fig. 5A) and the foot clearance (Fig. 5B) with the size of the obstacle. However, when an obstacle is crossed, the maximum knee flexion is larger for non-amputee participants than for above-knee participants using the powered prosthesis. Above-knee participants show smaller knee flexion but greater foot clearance than non-amputee participants (Fig. 5B). Furthermore, the variability of the maximum knee flexion decreases with the size of the obstacle for both the powered prosthesis and non-amputee tests (Fig. 5A). For the able-bodied group, the knee flexion and foot clearance during the treadmill tests match the knee flexion and foot clearance observed for the corresponding small obstacle test on level ground. With the powered prosthesis, the amputee group experienced a slight increase in knee flexion and clearance when crossing the small obstacle on the treadmill compared with when they crossed it on level ground. The maximum knee flexion and foot clearance of the passive prosthesis are much lower than the powered prosthesis and biological leg. Because of the lack of knee flexion, the passive prosthesis hits the obstacles for all tests and participants. In contrast, the foot clearance with the powered prosthesis volitional controller is sufficient to cross over obstacles up to 20 cm tall. Thus, non-amputee participants and individuals with amputations using the powered prosthesis show similar trends of maximum knee angle and foot clearance as a function of the obstacle size, although an offset between the two groups is observed.

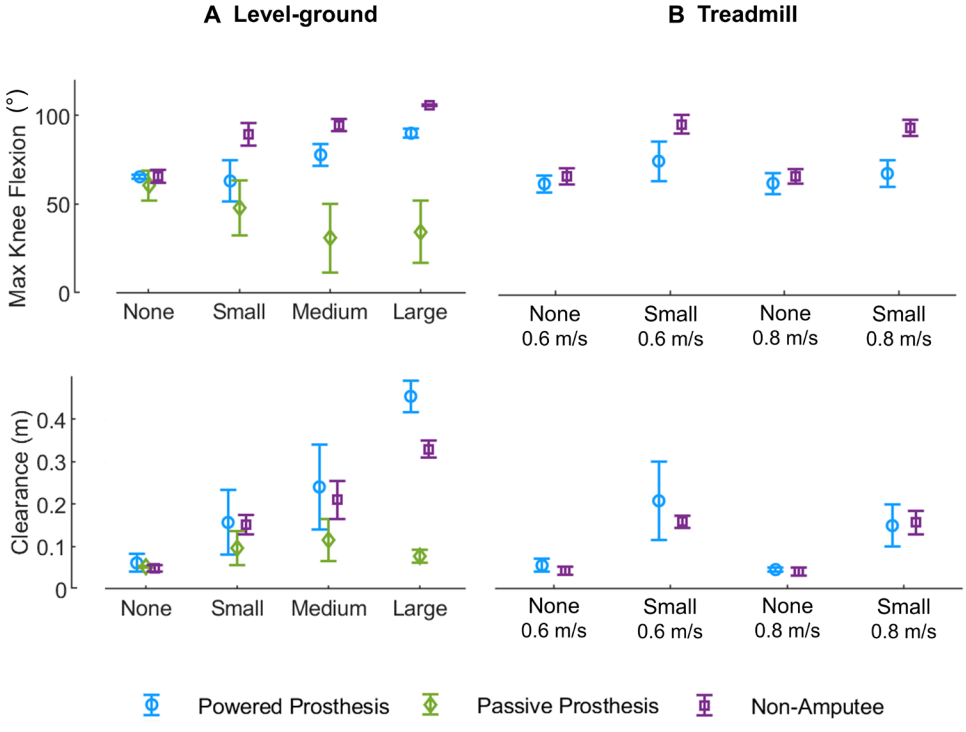

Fig. 5. Comparison between powered prosthesis, passive prosthesis, and non-amputee limb. (**A**) Max knee flexion and max foot clearance for level-ground tests. (**B**) Max knee flexion and max foot clearance for treadmill tests. Error bars represent the SD between the mean values of each participant within that group.

DISCUSSION

By actively regulating knee flexion during swing, powered prostheses have the potential to enable amputee individuals to traverse environmental barriers without using compensatory movements. Available controllers aim to achieve this goal by switching between different pre-planned swing trajectories that are appropriate to deal with different ambulation tasks (*25*). A previous study using a classifier to discriminate between regular walking and obstacle crossing with one amputee participant showed both low accuracy (i.e., 83%; ~one in five steps misclassified) and the inability to change the prosthesis knee flexion when dealing with obstacles (*32*). Another study with one amputee participant showed crossing over a small obstacle (i.e., 8.5 cm) with a powered prosthesis using hip

circumduction (*18*), which is the same compensatory movement used with passive prostheses (*35*). This study presents a fundamental departure from current control paradigms. Rather than aiming to classify the environmental barrier and switching between different, pre-planned swing trajectories, we propose to continuously modulate the trajectory of the powered prosthesis based on the movements of the user's residual limb so that environmental barriers can be negotiated without being classified. Our results suggest that this alternative paradigm can enable individuals with an above-knee amputation to ambulate on level ground at different speeds while seamlessly crossing over obstacles. This functionality is not currently available to prosthesis users and may lead to improved community ambulation. Our results also suggest that the proposed control strategy does not require collecting individual-specific datasets and manually tuning the controller for each individual and obstacle, which require knowledge and expertise not available to clinicians. For these reasons, the proposed control strategy may more easily translate into a clinical solution.

In agreement with previous studies, our experiments with three non-amputee participants (Fig. 4) show that crossing over an obstacle requires increasing both hip and knee flexion to shorten the limb and increase foot clearance (*36*). In addition, in agreement with previous studies, our experiments show that individuals with above-knee amputations using passive prostheses cannot cross over obstacles without ipsilateral hip circumduction (i.e., prosthesis side) and contralateral ankle plantarflexion (i.e., sound side vaulting) due to the lack of prosthesis knee flexion (*35*). Our controller can theoretically modulate foot clearance through two concomitant factors also observed in non-amputee individuals (Fig. 1). The first factor is the increase in maximum knee flexion. The second factor is the timing between the movements of the user's residual limb and the prosthetic knee, such as for the same thigh angle; the prosthesis knee flexion angle increases when crossing over obstacles. When obstacles are crossed on level ground (Fig. 4, B to D), both increased maximum knee flexion and the timing seem to factor into the observed increased of foot clearance. In contrast, when small obstacles are crossed at an imposed walking speed on the treadmill (Fig. 4, E and F), the timing of the thigh and knee movements seems to be the dominant factor determining foot clearance (table S1). This result differs for non-amputee participants, who visibly increase maximum knee flexion when crossing small obstacles on the treadmill (Fig. 4, B to D) For both amputee and non-amputee participants, strides with a higher clearance required a longer swing time, meaning that users spent an extended time on their contralateral, sound leg (Fig. 3). Amputee participants were generally slower than non-amputee participants, also spending more time in swing because the obstacle size increased (Fig. 3). Differences are also visible in the hip and thigh kinematics. The maximum thigh extension angle was visibly greater for the amputee group than the non-amputee group both in stance and swing (Fig. 4). In contrast, the maximum hip extension angle did not differ between the two groups (Fig. 4). This analysis suggests that the greater thigh extension was due to postural changes with the amputee participants leaning slightly forward with their trunk. This behavior is observed with both the powered and the passive prosthesis and during both stance and swing (Fig. 4). Thus, the observed increase of the thigh extension angle in the amputee group does not seem to be due to the proposed controller but rather a compensatory movement acquired by the amputee participants when using their passive prostheses. We speculate that this behavior may be the consequence of participants trying to shift their body weight on the leading leg (i.e., sound side) or trying to watch their feet and the obstacle while walking. Regardless, it is unclear whether the observed increase in the thigh extension angle is necessary to cross over the obstacles because foot clearance was generally higher in the amputee group than in the non-amputee group (Fig. 5).

Training is an important aspect that should be better investigated. In our experience, training is necessary for all ambulation activities including walking (with or without obstacles), climbing stairs, and performing sit-to-stand transitions. Although most participants can perform these activities from the outset of donning the powered prosthesis, they still need time and coaching to gain confidence, drop the compensatory movements used with their passive prostheses, and fully benefit from the increased functionality offered by the powered prosthesis. In this study, amputee participants performed about 20 rounds of each obstacle size on level ground and a few 2-min walking sessions on a treadmill. Our results suggest that this amount of practice may be sufficient to learn how to use the proposed volitional controller. However, it is not clear how the performance will change with further training because previous studies have shown that adapting to perform new tasks with a prosthesis can take up to 3 months of regular use (*37*). Different users may require a different amount of training to achieve the same level of proficiency. Participant-specific tuning of the controller was not necessary for this study, but it may be desirable to maximize outcomes as the user's proficiency with the prosthesis improves. Further exploration into the interaction between training, controller tuning, and gait performance should be conducted in the future.

The goal of this study is to show that continuous modulation of the prosthesis swing trajectory based on the residual limb can enable individuals with above-knee amputations to volitionally change foot clearance as necessary to traverse environmental barriers. Generalization of the proposed control paradigm is shown across three different participants ranging from 27 to 72 years old, four different obstacle conditions (0, 6, 10, and 20 cm), and two different terrains (over ground and treadmill). The combination of walking speeds and obstacle sizes tested in the final protocol was not part of the training session. A video of the experiment is available in the Supplementary Materials. Our study suggests that age may not be a factor in the user's ability to successfully use the proposed controller (table S2), although using a lightweight powered prosthesis (*38*, *39*) may have had an impact on this observation. Although volitional control over foot clearance may prevent certain stumble events to happen, it is unclear whether it would make recovering from a stumble easier or not. In general, the powered knee transitions to stance whenever it physically interacts with the environment, which causes the knee to fully extend at maximum speed and lock as it touches the ground. The current study sample is, however, too small to generalize the observed controller performance to the broader above-knee amputee population or to other ambulation tasks that may benefit from volitional control of foot clearance, such as walking on uneven or inclined terrains or reacting to stumble events. Future clinical studies should be conducted on a broader amputee population to assess the efficacy of the proposed intervention compared with the current standard of care for above-knee amputation.

Active control of joint position is one of the biggest advantages of powered prostheses over conventional passive devices. Safely walking at different speeds while navigating environmental barriers requires the prosthesis controller to generate unique swing trajectories

in synchrony with the user's movements. The proposed swing controller enables a powered prosthesis to adapt the swing trajectory continuously and smoothly without explicit classification of the environment. Providing users with volitional control over the knee flexion angle, the proposed controller allows for active modulation of foot clearance. Experiments with three individuals with above-knee amputations show that the proposed controller supports walking at different speeds and crossing over obstacles of different sizes without individual-specific tuning or explicit environment classification. A controller with this capability may improve community ambulation involving obstacles and uneven terrains and is not currently available to prosthesis users. Future work will be dedicated to evaluating the performance of the proposed controller in a larger clinical population and to assessing functional mobility compared with passive prostheses and powered prostheses using other control approaches.

MATERIALS AND METHODS

At the high level, the proposed controller uses a finite-state machine after (*11*). As can be seen in the block diagram of Fig. 6, the proposed finite-state machine composes of two stance states and two swing states. When the user is standing still, the prosthesis controller is in stance 1. If the ankle joint exceeds a dorsiflexion threshold ($\theta_{ankle} < \theta^{ths}_{ankle}$) and has positive plantar flexion velocity ($\dot{\theta}_{ankle} > 0$), then the system transitions to stance 2, which is an energy-injection state. From stance 2, the prosthesis transitions to swing 1 when the instrumented pyramid adapter (*40*) detects a ground reaction force (GRF) lower than 5% of the user's body weight. The stance states and the related transition conditions have been previously tested with individuals with an above-knee amputation (*38*). In swing 1, the knee joint flexes to increase foot clearance. In this state, the knee joint trajectory is modulated by the controller to continuously change the desired maximum knee flexion. From swing 1, the system transitions to swing 2 if the orientation of the user's residual limb exceeds a position threshold ($\theta_{thigh} < \theta^{ths}_{thigh}$) or if duration of swing 1 exceeds a time threshold ($t_{sw1} > T^{ths}_{sw1}$). In swing 2, a knee extension trajectory is programmed, enabling a timely placement of the prosthetic foot in preparation for the subsequent heel strike. Last, the prosthesis transitions from swing 2 to stance 1 if the instrumented pyramid adapter detects the GRF being higher than 5% of the user's body weight.

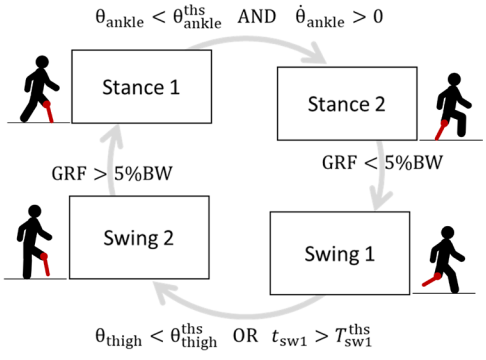

Fig. 6. Block diagram of the proposed finite-state machine. In stance 1, the prosthesis (red segment) absorbs the impact with the ground, storing and dissipating energy as necessary. The prosthesis transitions to stance 2 when the ankle position is greater than a specific dorsiflexion angle, and the ankle velocity is positive (i.e., the ankle is plantarflexing). When the instrumented pyramid detects the GRF being lower than 5% of the user's body weight (BW), the controller transitions to swing 1. In swing 1, the proposed controller adapts the prosthesis trajectory based on the movements of the residual limb. If the residual limb exceeds a variable threshold, then the prosthesis switches to swing 2, where a minimum-jerk trajectory is generated to prepare the foot for the subsequent heel strike.

The orientation of the user's residual limb drives the adaptation of the desired knee trajectory in swing 1. As shown in the block diagram of Fig. 7, the desired maximum knee flexion angle (θ^{des}_{final}) in swing 1 is determined by the integral of the residual limb orientation with respect to gravity (θ_{thigh}), computed from the start to the end of swing 1 (Fig. 6), according to Eq. 1

$$\theta^{des}_{final}(t) = K_1 + K_2 \int_0^{T_{sw1}} (\theta_{thigh}(t) + K_3)\, dt \quad (1)$$

Three parameters affect the desired maximum knee flexion angle (θ^{des}_{final}). The first parameter is a constant (i.e., $K_1 = 55$) that determines the desired angle at the start of the swing movement, when the integral output is zero. The second parameter is a gain (i.e., $K_2 = 2$) that affects the sensitivity of the integral. The third parameter (i.e., $K_3 = 20$) is a constant added to the thigh angle (θ_{thigh}), which provides a bias for the output of the integral. This bias term is used to ensure that the integral increases continuously throughout swing, as the position values for thigh extension ($\theta_{thigh} > 0$) negate those for thigh flexion ($\theta_{thigh} < 0$). These three fixed parameters are determined from both the analysis of non-amputee biomechanics and pilot testing with individuals with amputations. The same parameters are used for all participants. Combined, the parameters K_1 and K_2 allow the controller to approximate the range of knee flexion observed in non-amputee individuals in different scenarios (table S1). A high initial flexion angle, K_1, with and a low sensitivity, K_2, can result in a physiological knee flexion for regular walking but fail to provide the necessary increase in knee flexion needed to obtain larger clearance when crossing obstacles. Similarly, a low initial flexion angle, K_1, and a high sensitivity, K_2 , can result in exaggerated knee flexion, which can potentially be unsafe for users. Because of the proposed heuristic algorithm (Eq. 1), the desired maximum knee flexion angle (θ^{des}_{final}) increases when the residual limb is positioned farther back or when it is slowly moved forward during swing 1 (i.e., right after toe-off). Thus, the prosthesis knee swing trajectory can theoretically be modulated by the users through their residual limb, potentially enabling variable foot clearance.

Given a desired maximum knee flexion angle (θ^{des}_{final}), the swing trajectory is continuously optimized using minimum jerk. As shown in the block diagram of Fig. 7, the minimum-jerk planner takes as input the desired maximum knee flexion angle (θ^{des}_{final}) and the desired movement duration (T^{des}_{final}), which is computed in swing 1 by subtracting the current swing time [$t_{sw1}(t)$] from the desired swing 1 duration (T_{sw1}), as shown by Eq. 2

$$T^{des}_{final}(t) = T_{sw1} - t_{sw1}(t) \quad (2)$$

On the basis of these two inputs and the previous desired position, velocity, and acceleration, the minimum-jerk planner updates the desired swing trajectory by computing the desired angle, velocity, and acceleration of the knee joint. The desired angle, velocity, and acceleration are then passed to a mixed feedforward/feedback regulator that determines the desired torque at the knee joint level (Fig. 7). A new trajectory can branch off from the swing trajectory

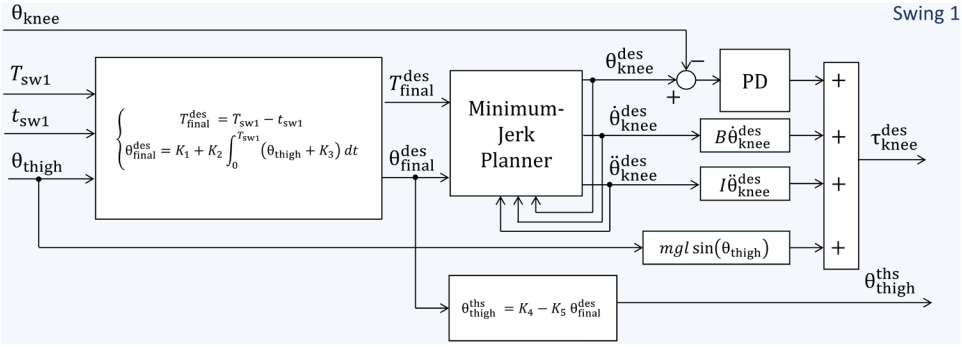

Fig. 7. Block diagram representation of the proposed adaptive controller used in swing 1. The desired knee angle at the end of swing 1 (θ^{des}_{final}) is continuously updated on the basis of the orientation of the user's residual limb with respect to gravity (θ_{thigh}) using an integral function (Eq. 1). On the basis of the desired knee angle (θ^{des}_{final}) and the remaining time in swing 1 (T^{des}_{final}), the minimum-jerk planner computes the desired knee angle trajectory (θ^{des}_{knee}, $\dot{\theta}^{des}_{knee}$, $\ddot{\theta}^{des}_{knee}$), which is then passed to a closed-loop position controller including a proportional-derivative (PD) regulator and feedforward compensators for viscosity and inertia. In addition, the threshold for transitioning between swing 1 and swing 2 (θ^{ths}_{thigh}) is updated on the basis of the desired knee angle (θ^{des}_{final}) and passed on to the finite-state machine.

originally programmed at toe-off if the desired final position or the desired swing duration changes. Thus, with the proposed continuous minimum-jerk planning, the prosthesis can smoothly change the swing trajectory while it is being performed regardless of the current angle, velocity, and acceleration of the prosthesis joint.

Although the desired maximum knee flexion (θ^{des}_{final}) is computed through the integral of the residual limb orientation (θ_{thigh}), the actual peak of knee flexion depends on the position of the knee at the transition between swing 1 and swing 2. The finite-state machine transitions from swing 1 to swing 2 when the thigh angle (θ_{thigh}) exceeds a threshold (θ^{ths}_{thigh}) (Fig. 6). However, this threshold is not fixed but rather varies as a function of the desired peak knee flexion (θ^{des}_{final}) as defined by Eq. 3, where $K_4 = 17.5$ and $K_5 = 0.5$. The values of K_4 and K_5 are determined offline to imitate the kinematics of non-amputee individuals (Fig. 4). Specifically, K_4 is set to serve as an offset for the thigh threshold (θ^{ths}_{thigh}), and K_5 serves as the sensitivity of the thigh threshold (θ^{ths}_{thigh}) to the desired knee flexion (θ^{des}_{final}), which is determined using Eq. 1

$$\theta^{ths}_{thigh}(t) = K_4 - K_5\,\theta^{des}_{final}(t) \quad (3)$$

On the basis of Eq. 3, the thigh threshold at the transition between swing 1 and swing 2 increases proportionally to the desired peak knee flexion (θ^{des}_{final}). Thus, the transition between swing 1 and swing 2 can happen at different points within the swing, although the desired duration of swing 1 (T_{sw1}) is constant at 0.4 s.

In swing 2, the prosthesis uses a minimum-jerk controller to ensure timely placement of the foot in preparation for the subsequent heel strike. Although there is no continuous adaptation of the prosthesis trajectory during this phase, using the minimum-jerk planner in swing 2 is crucial to obtain the desired controller behavior. As shown by the simulation results of Fig. 1, the system can transition to swing 2 with different knee positions and velocities (dot markers of different colors). As a result, the desired trajectory in swing 2 may allow for both knee flexion and extension, effectively modulating the maximum knee flexion achieved by the powered prosthesis in the swing. This controller behavior contrasts with previous controllers, where swing 2 is used for knee extension only (*11*, *17*, *18*, *35*).

In stance, we use a control framework previously tested with individuals with above-knee amputations (*17*). This stance controller enforces physiological torque-angle curves extracted from non-amputee individuals walking at different speeds (*16*). Thus, the knee and ankle torque profiles are adapted online on the basis of the respective joint positions and an overall estimate of the current walking speed. Different from impedance-based controllers, this stance controller does not require user-specific or speed-specific tuning. However, the body weight of the user must be inserted in the controller by the experimenter through a graphical user interface. Although we use this stance control strategy, the proposed swing controller can be used with other stance controllers because any initial angle, speed, and acceleration can be handled by the minimum-jerk swing controller.

A longer stride and a larger knee flexion are shown to produce a higher clearance in non-amputee individuals. As a result, the proposed controller was developed around the volitional movement of the user's residual limb. Specifically, the controller continuously modulates the maximum knee flexion in swing depending on how far back the residual limb (i.e., thigh angle) is positioned and how fast the user moves it forward during the flexion part of swing (Eq. 1). Moreover, it was designed to adjust swing 1 duration (Fig. 6) because non-amputee individuals typically wait to start extension at a higher thigh angle whenever a higher clearance is desired. This heuristic adaptation of maximum knee flexion and swing 1 duration is combined with minimum-jerk programming to obtain a smooth behavior of the leg that qualitatively matches the behavior of the healthy leg. Minimum-jerk programming has been previously used for both powered knee and ankle prostheses to plan a smooth swing movement (*17*, *22*–*24*, *32*, *38*, *41*, *42*). However, in these previous studies, the minimum-jerk trajectory is programmed at toe-off and kept constant through the whole swing duration. Thus, the swing trajectory cannot be modified as necessary to cross over obstacles. In contrast, our continuous minimum-jerk planner updates the swing trajectory at every instance within the swing phase.

SUPPLEMENTARY MATERIALS

robotics.sciencemag.org/cgi/content/full/5/44/eaba6635/DC1

Materials and Methods

Fig. S1. Foot clearance is defined as the distance between the foot and the ground in the vertical (*y*) axis.

Fig. S2. The Utah lightweight leg comptises powered ankle and knee modules, each having one actuated degree of freedom in the sagittal plane.

Table S1. Group averages of the maximum knee flexion, thigh range, hip range, maximum clearance, and stride duration for all tested conditions.

Table S2. Subject data.

Movie S1. Example experiment showing one participant walking and crossing over obstacles.

REFERENCES AND NOTES

1. D. Berry, Microprocessor prosthetic knees. *Phys. Med. Rehabil. Clin. N. Am.* **17**, 91–113 (2006).
2. J. W. Michael, Modern prosthetic knee mechanisms. *Clin. Orthop. Relat. Res.* **361**, 39–47 (1999).

3. J. L. Johansson, D. M. Sherrill, P. O. Riley, P. Bonato, H. Herr, A clinical comparison of variable-damping and mechanically passive prosthetic knee devices. *Am. J. Phys. Med. Rehabil.* **84**, 563–575 (2005).
4. B. J. Hafner, L. L. Willingham, N. C. Buell, K. J. Allyn, D. G. Smith, Evaluation of function, performance, and preference as transfemoral amputees transition from mechanical to microprocessor control of the prosthetic knee. *Arch. Phys. Med. Rehabil.* **88**, 207–217 (2007).
5. M. B. Taylor, E. Clark, E. A. Offord, C. Baxter, A comparison of energy expenditure by a high level trans-femoral amputee using the Intelligent Prosthesis and conventionally damped prosthetic limbs. *Prosthet. Orthot. Int.* **20**, 116–121 (1996).
6. J. G. Buckley, W. D. Spence, S. E. Solomonidis, Energy cost of walking: Comparison of "intelligent prosthesis" with conventional mechanism. *Arch. Phys. Med. Rehabil.* **78**, 330–333 (1997).
7. T. Schmalz, S. Blumentritt, R. Jarasch, Energy expenditure and biomechanical characteristics of lower limb amputee gait: The influence of prosthetic alignment and different prosthetic components. *Gait Posture* **16**, 255–263 (2002).
8. D. A. Winter, S. E. Sienko, Biomechanics of below-knee amputee gait. *J. Biomech.* **21**, 361–367 (1988).
9. M. Schaarschmidt, S. W. Lipfert, C. Meier-Gratz, H.-C. Scholle, A. Seyfarth, Functional gait asymmetry of unilateral transfemoral amputees. *Hum. Mov. Sci.* **31**, 907–917 (2012).
10. H. Bateni, S. J. Olney, Kinematic and kinetic variations of below-knee amputee gait. *J. Prosthetics Orthot.* **14**, 2–10 (2002).
11. B. E. Lawson, J. Mitchell, D. Truex, A. Shultz, E. Ledoux, M. Goldfarb, A robotic leg prosthesis: Design, control, and implementation. *IEEE Robot. Autom. Mag.* **21**, 70–81 (2014).
12. A. M. Simon, N. P. Fey, S. B. Finucane, R. D. Lipschutz, L. J. Hargrove, Strategies to reduce the configuration time for a powered knee and ankle prosthesis across multiple ambulation modes. *IEEE Int. Conf. Rehabil. Robot.* **2013**, 6650371 (2013).
13. A. M. Simon, K. A. Ingraham, N. P. Fey, S. B. Finucane, R. D. Lipschutz, A. J. Young, L. J. Hargrove, Configuring a powered knee and ankle prosthesis for transfemoral amputees within five specific ambulation modes. *PLOS ONE* **9**, e99387 (2014).
14. F. Sup, H. A. Varol, J. Mitchell, T. J. Withrow, M. Goldfarb, Preliminary evaluations of a self-contained anthropomorphic transfemoral prosthesis. *IEEE ASME Trans. Mechatron.* **14**, 667–676 (2009).
15. H. Huang, D. L. Crouch, M. Liu, G. S. Sawicki, D. Wang, A cyber expert system for auto-tuning powered prosthesis impedance control parameters. *Ann. Biomed. Eng.* **44**, 1613–1624 (2016).
16. T. Lenzi, L. Hargrove, J. W. Sensinger, Preliminary evaluation of a new control approach to achieve speed adaptation in robotic transfemoral prostheses, in *2014 IEEE/RSJ International Conference on Intelligent Robots and Systems* (IEEE, 2014), pp. 2049–2054.
17. T. Lenzi, L. Hargrove, J. Sensinger, Speed-adaptation mechanism: Robotic prostheses can actively regulate joint torque. *IEEE Robot. Autom. Mag.* **21**, 94–107 (2014).
18. S. Rezazadeh, D. Quintero, N. Divekar, E. Reznick, L. Gray, R. D. Gregg, A phase variable approach for improved rhythmic and non-rhythmic control of a powered knee-ankle prosthesis. *IEEE Access* **7**, 109840–109855 (2019).
19. A. W. Boehler, K. W. Hollander, T. G. Sugar, D. Shin, Design, implementation and test results of a robust control method for a powered ankle foot orthosis (AFO), in *Proceedings of the IEEE International Conference on Robotics and Automation* (IEEE, 2008), pp. 2025–2030.
20. T. Lenzi, L. J. Hargrove, J. W. Sensinger, Minimum jerk swing control allows variable cadence in powered transfemoral prostheses, in *2014 36th Annual International Conference of the IEEE Engineering in Medicine and Biology Society* (IEEE, 2014), pp. 2492–2495.
21. B. Lawson, H. A. Varol, A. Huff, E. Erdemir, M. Goldfarb, Control of stair ascent and descent with a powered transfemoral prosthesis. *IEEE Trans. Neural Syst. Rehabil. Eng.* **21**, 466–473 (2013).
22. T. Lenzi, M. Cempini, L. J. Hargrove, T. A. Kuiken, Design, development, and validation of a lightweight non-backdrivable robotic ankle prosthesis. *IEEE/ASME Trans. Mechatronics* **24**, 471–482 (2019).
23. T. Lenzi, M. Cempini, L. Hargrove, T. Kuiken, Design, development, and testing of a lightweight hybrid robotic knee prosthesis. *Int. J. Rob. Res.* **37**, 953–976 (2018).
24. T. Lenzi, J. Sensinger, J. Lipsey, L. Hargrove, T. Kuiken, Design and preliminary testing of the RIC hybrid knee prosthesis, in *2015 37th Annual International Conference of the IEEE Engineering in Medicine and Biology Society (EMBC)* (IEEE, 2015), vol. 2015-Novem, pp. 1683–1686.
25. J. A. Spanias, A. M. Simon, S. B. Finucane, E. J. Perreault, L. J. Hargrove, Online adaptive neural control of a robotic lower limb prosthesis. *J. Neural Eng.* **15**, 016015 (2018).
26. H. Huang, F. Zhang, L. J. Hargrove, Z. Dou, D. R. Rogers, K. B. Englehart, Continuous locomotion-mode identification for prosthetic legs based on neuromuscular–mechanical fusion. *I.E.E.E. Trans. Biomed. Eng.* **58**, 2867–2875 (2011).
27. L. J. Hargrove, A. J. Young, A. M. Simon, N. P. Fey, R. D. Lipschutz, S. B. Finucane, E. G. Halsne, K. A. Ingraham, T. A. Kuiken, Intuitive control of a powered prosthetic leg during ambulation: A randomized clinical trial. *JAMA* **313**, 2244–2252 (2015).
28. M. H. Jahanandish, K. G. Rabe, N. P. Fey, K. Hoyt, Gait phase identification during level, incline and decline ambulation tasks using portable sonomyographic sensing, in *2019 IEEE 16th International Conference on Rehabilitation Robotics (ICORR)* (IEEE, 2019), pp. 988–993.
29. M. Liu, D. Wang, H. Helen Huang, Development of an environment-aware locomotion mode recognition system for powered lower limb prostheses. *IEEE Trans. Neural Syst. Rehabil. Eng.* **24**, 434–443 (2016).
30. N. E. Krausz, T. Lenzi, L. J. Hargrove, Depth sensing for improved control of lower limb prostheses. *I.E.E.E. Trans. Biomed. Eng.* **62**, 2576–2587 (2015).
31. N. Thatte, N. Srinivasan, H. Geyer, Real-time reactive trip avoidance for powered transfemoral prostheses, in *Robotics: Science and Systems XV* (Robotics: Science and Systems Foundation, 2019).
32. M. Gordon, N. Thatte, H. Geyer, Online learning for proactive obstacle avoidance with powered transfemoral prostheses, in *2019 International Conference on Robotics and Automation (ICRA)* (IEEE, 2019), pp. 7920–7925.
33. F. Zhang, M. Liu, H. Huang, Effects of locomotion mode recognition errors on volitional control of powered above-knee prostheses. *IEEE Trans. Neural Syst. Rehabil. Eng.* **23**, 64–72 (2015).
34. J. A. Spanias, E. J. Perreault, L. J. Hargrove, Detection of and compensation for EMG disturbances for powered lower limb prosthesis control. *IEEE Trans. Neural Syst. Rehabil. Eng.* **24**, 226–234 (2016).
35. A. H. Vrieling, H. G. van Keeken, T. Schoppen, E. Otten, J. P. K. Halbertsma, A. L. Hof, K. Postema, Obstacle crossing in lower limb amputees. *Gait Posture* **26**, 587–594 (2007).
36. L.-S. Chou, L. F. Draganich, Stepping over an obstacle increases the motions and moments of the joints of the trailing limb in young adults. *J. Biomech.* **30**, 331–337 (1997).
37. T. Schmalz, M. Bellmann, E. Proebsting, S. Blumentritt, Effects of adaptation to a functionally new prosthetic lower-limb component: Results of biomechanical tests immediately after fitting and after 3 months of use. *J. Prosthetics Orthot.* **26**, 134–143 (2014).
38. M. Tran, L. Gabert, M. Cempini, T. Lenzi, A lightweight, efficient fully powered knee prosthesis with actively variable transmission. *IEEE Robot. Autom. Lett.* **4**, 1186–1193 (2019).
39. L. Gabert, S. Hood, M. Tran, M. Cempini, T. Lenzi, A compact, lightweight robotic ankle-foot prosthesis: Featuring a powered polycentric design. *IEEE Robot. Autom. Mag.* **27**, 87–102 (2020).
40. L. Gabert, T. Lenzi, Instrumented pyramid adapter for amputee gait analysis and powered prosthesis control. *IEEE Sens. J.* **19**, 8272–8282 (2019).
41. M. Cempini, L. J. Hargrove, T. Lenzi, Design, development, and bench-top testing of a powered polycentric ankle prosthesis, in *IEEE/RSJ International Conference on Intelligent Robots and System* (IEEE, 2017), vol. 2017-Septe, pp. 1064–1069.
42. N. Thatte, T. Shah, H. Geyer, Robust and adaptive lower limb prosthesis stance control via extended kalman filter-based gait phase estimation. *IEEE Robot. Autom. Lett.* **4**, 3129–3136 (2019).

Acknowledgments: We would like to thank M. Tran and L. Gabert for help with the development of the prosthesis hardware and software components. We would also like to thank M. Ishmael for helping with human studies. We would like to thank K. Rasmussen, CPO for help with prosthesis fitting. **Funding:** This work was partly supported by the NIH under grant number 1R01HD098154-01A1 and the NSF under grant number 1925371. **Author contributions:** T.L. directed the project. T.L. and J.M. invented the controller and implemented it on the Utah lightweight leg for the purpose of the experiments. J.M., S.H., T.L., and A.G. conducted the experiments with human participants. J.M. and A.G. analyzed the data. All authors contributed to the manuscript preparation. **Competing interests:** The authors declare that they have no financial interests. T.L. is an inventor of the following awarded patents related to this study: "Powered and passive assistive device and related methods" (U.S. Patent no. 10,357,381, 23 July 2019) and "Minimum Jerk Swing Control for Assistive Device" (U.S. Patent no. 10,213,324.B2). **Data and materials availability:** All data needed to evaluate the conclusions in the paper are present in the paper or the Supplementary Materials.

Submitted 21 December 2019
Accepted 25 June 2020
Published 22 July 2020
10.1126/scirobotics.aba6635

Citation: J. Mendez, S. Hood, A. Gunnel, T. Lenzi, Powered knee and ankle prosthesis with indirect volitional swing control enables level-ground walking and crossing over obstacles. *Sci. Robot.* **5**, eaba6635 (2020).

Science Robotics

Powered knee and ankle prosthesis with indirect volitional swing control enables level-ground walking and crossing over obstacles

Joel Mendez, Sarah Hood, Andy Gunnel, and Tommaso Lenzi

Sci. Robot. **5** (44), eaba6635. DOI: 10.1126/scirobotics.aba6635

Science Robotics (ISSN 2470-9476) is published by the American Association for the Advancement of Science. 1200 New York Avenue NW, Washington, DC 20005. The title *Science Robotics* is a registered trademark of AAAS.